Electronic Supplementary Material (ESI) for ChemComm.

Mesoporous Titanium and Niobium Nitrides as Conductive and Stable Electrocatalyst Supports in Acid Environments

Materials

Tetrahydrofuran (THF, ≥ 99.9% inhibitor-free, anhydrous), 1-butanol (99.8%, anhydrous), toluene (99.8%, anhydrous), ferrocenemethanol (97%), ethanol (absolute, ≥ 99.8%), chloroplatinic acid hexahydrate (ACS reagent, ≥ 37.50% Pt basis), Nafion 117 solution (~5% mixture of lower aliphatic alcohols and water), and titanium wire (99.99%) were obtained from Sigma Aldrich and used as received. Niobium (V) ethoxide (99.999% metals basis) and titanium (IV) isopropoxide (99.999% trace metals basis) were obtained from Alfa Aesar and used as received. Argon (ultra-high purity), oxygen (ultra-high purity), 5% hydrogen in nitrogen (certified standard), and ammonia (99.9%; anhydrous, premium grade) were obtained from Airgas. Argon, H_2/N_2, and oxygen were used as received, while ammonia was purified over a SAES MicroTorr MC400-702F purifier to remove residual oxygen and moisture.

Hydrochloric acid (37wt%; American Chemical Society/National Formulary/Food Chemicals Codex grade) and perchloric acid (GFS Chemicals, Veritas double-distilled) were used as received. Silver paint (Leitsilber 200) was obtained from Ted Pella while Omegabond 101 epoxy was obtained from Omega Engineering. Isopropyl alcohol (99%) was obtained from BDH and used as received. All aqueous solutions were prepared using 18.2 MΩ water from a Direct-Q system (Millipore).

For polymer synthesis, sec-butyl lithium (1.4M in cyclohexane), n-butyl lithium (1.6M in hexanes), naphthalene (99%) and potassium chloride (99.999%) were obtained from Sigma Aldrich and used as received. Other chemicals used as received include: chloroform (J.T. Baker, 99%), potassium (Fluka, 98%), methanol (Mallinckrodt, ACS), and diphenylethylene (Acros, 99%). Isoprene (Aldrich, 99%) and ethylene oxide (Aldrich, ≥ 99.5%) were distilled from n-butyl lithium prior to use. Benzene (EMD Millipore, 99%) and tetrahydrofuran (Mallinckrodt, 99%) were distilled from n-buytl lithium and diphenylethylene prior to use. Styrene was distilled from calcium hydride prior to use. Methanolic HCl (Supelco, 3N) was degassed via a standard freeze-pump-thaw method prior to use.

Polymer Synthesis

An 86 kg/mol poly(isoprene)-block-poly(styrene)-block-poly(ethylene oxide) (PI-b-PS-b-PEO, or simply ISO) triblock terpolymer was prepared via sequential anionic polymerization using known procedures.[1,2] The ISO terpolymer was composed of polyisoprene 22.7 kg/mol, polystyrene 58.7 kg/mol, and poly(ethylene oxide) 4.7 kg/ mol with a polydispersity index of 1.09.

It should be noted that sec- and n-butyl lithiums are pyrophoric and ethylene oxide is highly toxic and extremely reactive. Briefly, sec-butyl lithium was added to vacuum-distilled benzene in a Schlenk flask. Isoprene was distilled from n-butyllithium and added to the Schlenk flask in a nitrogen glovebox, and allowed to stir for ~12 hours. Styrene was distilled from calcium hydride, added likewise, and allowed to stir for ~12 hours. To endcap the polymer with a single ethylene oxide unit, ethylene oxide was double-distilled from n-butyl lithium and added via reverse injection on a Schlenk line. The polymer was then terminated by addition of degassed methanolic HCl, dried, redissolved in chloroform, washed three times with deionized water, and precipitated into ~10 volumes of cold methanol. The ethylene-

hydroxide-terminated poly(isoprene-b-styrene) was then dried under vacuum on a Schlenk line for ~5 days at temperatures up to 130 ˚C. Tetrahydrofuran was then distilled onto the dry polymer and potassium naphthalenide titrated to re-initiate to polymer in a nitrogen glovebox. Ethylene oxide was again double-distilled from n-butyllithium and added. The reaction was allowed to stir at 40 ˚C for 4 days before termination with degassed methanolic HCl. The solvent was then removed, polymer redissolved in chloroform, washed three times with deionized water, precipitated into cold methanol, and vacuum-dried at 50 ˚C. Terpolymer molar mass and block fractions were determined by a combination of ^{1}H nuclear magnetic resonance spectroscopy and gel permeation chromatography.

Mesoporous NbN Thin Film Synthesis

The mesoporous NbN thin film synthesis is based on a modified literature procedure for NbN mesoporous monoliths.[3] In a typical synthesis, 50 mg of ISO terpolymer was dissolved under stirring in 0.875 mL of anhydrous THF. The Nb_2O_5 sol was synthesized by first preparing a solution of 0.15 mL HCl and 0.5 mL THF and stirring for 10 minutes. Subsequently, 0.255 mL of niobium (V) ethoxide was added and allowed to react under vigorous stirring for five minutes. An additional 0.5 mL of anhydrous THF was then added to quench the reaction and the solution was stirred for two additional minutes. A 0.155 mL aliquot was added to 50 mg of the terpolymer solution and stirred overnight.

Silicon wafers with a 3 μm thermal oxide were cleaved into ~1cm^2 pieces using a diamond scribe and cleaned three times each in de-ionized water, acetone, and THF. Films were then spin cast in an N_2-purged drybox with < 20% relative humidity at 2,000 rpm for 45 s. Following spin-casting, films were solvent annealed at 35 °C under a glass dome in a THF-saturated environment for 48 h. Subsequently, the films were dried in a vacuum oven at 130 °C for 3 h. Subsequent heating at 450 °C for 3 h in air (1 °C/min ramp rate) removed all organic components and an amorphous Nb_2O_5 mesoporous structure was formed. This oxide was heated under flowing ammonia at 700 °C for 12 hours (2.5 L/hr, 5 °C/min ramp rate) to form rock salt NbN and then cooled to room temperature under NH_3.

Mesoporous TiN Thin Film Synthesis

The mesoporous TiN thin film synthesis is based on a modified literature procedure for mesoporous TiN-containing monoliths.[4] In a typical synthesis, 50 mg of ISO terpolymer was dissolved in 0.75 mL of anhydrous THF. The TiO_2 sol was synthesized by adding 0.5 mL of titanium (IV) isopropoxide to 0.15 mL HCl under vigorous stirring for 5 minutes. Then 1 mL anhydrous THF was added and the solution was stirred for two additional minutes. A 0.275 mL aliquot was added to 50 mg of the terpolymer solution and stirred overnight. The TiO_2/terpolymer solution was then spin cast and annealed under the same conditions as the Nb-based system.

Platinum Nanoparticle Incorporation into TiN Films

Platinum nanoparticles were incorporated into TiN films by first preparing a 1 mg/mL solution of chloroplatinic acid hexahydrate in ethanol. The solution was dropcast onto a TiN film such that a final film composition of 10 wt% Pt/TiN was achieved. The film was then allowed to dry overnight. After drying, the Pt was reduced under 5% H_2/N_2 at 150 °C (2.5 L/hr, 5 °C/min ramp) for 2 h. Upon cooling, Nafion 117 was dropcast onto the film to adhere the nanoparticles to the support. The amount of Nafion was chosen such that a 1 nm coating of the pore walls was achieved, assuming conformal coating.

XRD Characterization

A Rigaku Ultima IV diffractometer equipped with a D/teX Ultra detector using CuK_{α} radiation was used to obtain powder diffraction data for each oxide and nitride in this study. Crystallite size was obtained for the nitride samples using Debye-Scherrer analysis by averaging the peak width of all peaks between 30° and 70°, while lattice parameters were calculated from $2d_{200}$ for each material.

After the ISO terpolymer is removed, an amorphous niobium oxide is formed. For the Ti-based system, however, anatase TiO_2 is formed upon heating in air. These results are consistent with literature showing a lower crystallization temperature for TiO_2[5] than Nb_2O_5.[6]

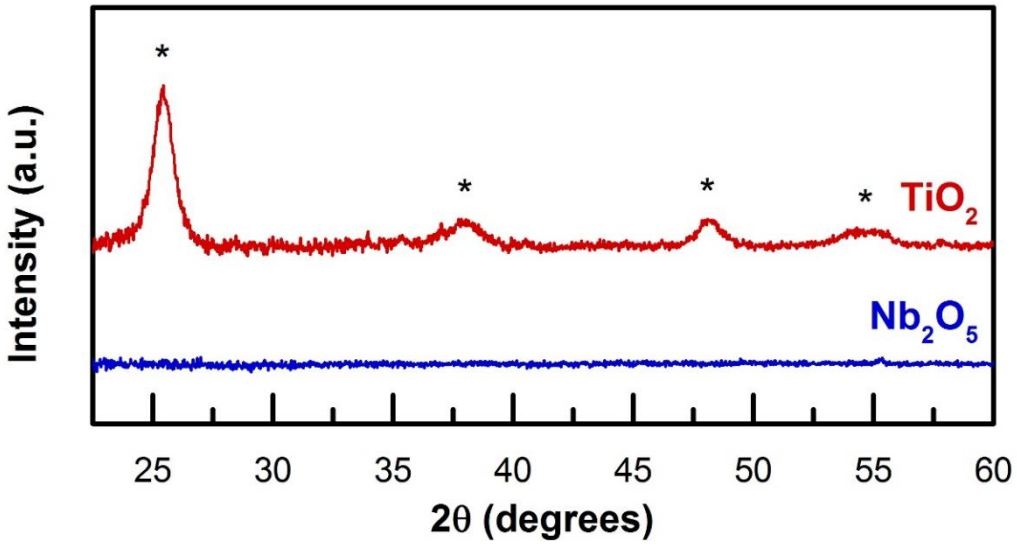

Figure S1: X-ray diffraction spectra after heating oxide/terpolymer hybrid in air at 450 °C for 3 hours. The TiO_2 film shows peaks consistent with the anatase phase while the Nb-based film is amorphous.

Electrochemical Testing

Electrodes were fabricated by adhering titanium wire to the nitride films both with and without Pt. First, the wires were polished to remove the surface oxide and then they were subsequently affixed to the films as top contacts with conductive silver paint and allowed to cure for 2 h. After curing, an inert two-part epoxy was mixed and used to cover the back and sides of the substrate as well as the silver paint and approximately 1 inch of the wire to ensure that only the nitride film generated an electrochemical response. The inert epoxy was allowed to cure for 12 h.

All electrochemical measurements were conducted using a three-electrode electrochemical cell (Pine) with 0.1 M $HClO_4$ as the supporting electrolyte and a platinum wire as the counter electrode. The applied potential was controlled using a Bio-Logic SP-300 potentiostat while an Ag/AgCl electrode (Pine) was used as the reference electrode. The reference electrode was placed in a capillary filled with 0.1 M $HClO_4$ to further isolate it from the electrolyte and prevent chlorine evolution at high applied potentials. The reference electrode was calibrated against the reversible hydrogen electrode (RHE) scale by measuring the hydrogen evolution/oxidation currents on a polycrystalline Pt disk (Pine) in 0.1 M $HClO_4$ electrolyte. The cell was saturated with hydrogen (Airgas, ultra-high purity) and the potential where the current was zero was assigned as 0 V vs. RHE, in this case 0.263 mV vs. Ag/AgCl. All the potentials in this study were referenced to the RHE potential scale and correspond to the iR-corrected potentials, E_{iR-}

$_{corrected}$, calculated with $E_{iR\text{-}corrected} = E_{applied} - iR$ where $E_{applied}$ is the voltage applied from the potentiostat, i is the current and R is the uncompensated ohmic electrolyte resistance. The electrolyte resistance, R, was measured as the AC impedance at high frequency of the three-electrode system.

Capacitance measurements of all films were obtained using cyclic voltammetry in an electrolyte saturated with argon (Airgas, ultra-high purity) prior to measurement. To measure the redox conductivity of the films, 300 μM ferrocenemethanol was added to the electrolyte and stirred vigorously overnight prior to saturating the electrolyte with argon and performing cyclic voltammetry.

Electrochemical Stability Analysis:

To evaluate the electrochemical stability window of TiN and NbN, films were cycled at 50 mV/s in Ar-saturated 0.1 M $HClO_4$. For the purposes of this study, electrochemical stability is defined as the potential range where the capacitance and conductivity are stable. The upper potential window limit for NbN can be seen in Fig S9, where subjecting NbN to potentials above 0.85 V vs. RHE resulted in an irreversible loss in capacitance and elimination of the Fe^{2+}/Fe^{3+} redox peaks, an outer-sphere redox couple that was used to assess the material's conductivity (Fig S8b). Meanwhile, TiN does not show any conductivity loss up to at least 1.4 V vs. RHE (Fig S8a, Fig S10), indicating that it is more stable against oxidative potentials than NbN and can be tested in a wider potential window than NbN.

Further, we evaluate the long-term stability by cycling the nitride support between 0.5 and 1.4 V vs. RHE at 50 mV/s. After 100, 200, 500, 1,000, 1,500, and 2,000 cycles, we measure a CV from 0.1 to 1.4 V vs. RHE at 50 mV/s to quantify the capacitance. In this communication, we are focused on support degradation so assessing the long-term stability of TiN in the absence of Pt particles provides a more direct probe of the support stability. A stability test of the nitrides in the presence of Pt can be confounded by Pt dissolution, which is a major degradation mechanism of Pt, but not of the support.[7,8]

Platinum Nanoparticle Cyclic Voltammetry:

The viability of TiN as a catalyst support was further investigated by incorporating Pt nanoparticles. These Pt/TiN films were cycled at 50 mV/s in Ar-saturated 0.1 M $HClO_4$. An electrochemically active surface area (ECSA) of 47.6 m^2/g was calculated by integrating the area under the hydrogen adsorption peaks. This ECSA is comparable to heat-treated commercial Pt catalysts (Tanaka or TKK[7], Johnson Matthey[9], and E-TEK[10]), indicating a good dispersion. A poor dispersion would result in lowering of the ECSA well below these commercial catalysts as a result of larger particles dominating the ECSA value.

GISAXS Results:

Grazing incidence small angle X-ray scattering (GISAXS) data were collected at station G1 of the Cornell High Energy Synchrotron Source (CHESS), with an incident beam energy of 11.3 keV and a typical sample-to-detector distance of 2 m. Data were taken at an incident angle between the critical angles of the film and the silicon substrate, approximately 0.12°. Two-dimensional GISAXS patterns were recorded on a Dectris EIGER 1M pixel-array detector, normalized, and processed using the Nika software package for Igor Pro.[11] GISAXS data were integrated in horizontal lines just above or below the reflected band to produce the line profiles shown in Figure 2. For all four samples the integration width was $\pm$ 0.005 A^{-1}. For TiO_2 the integration was about $q_z = 0.024$ A^{-1}, for TiN $q_z = 0.023$ A^{-1}, for Nb_2O_5 $q_z = 0.035$ A^{-1}, and for NbN $q_z = 0.034$ A^{-1}.

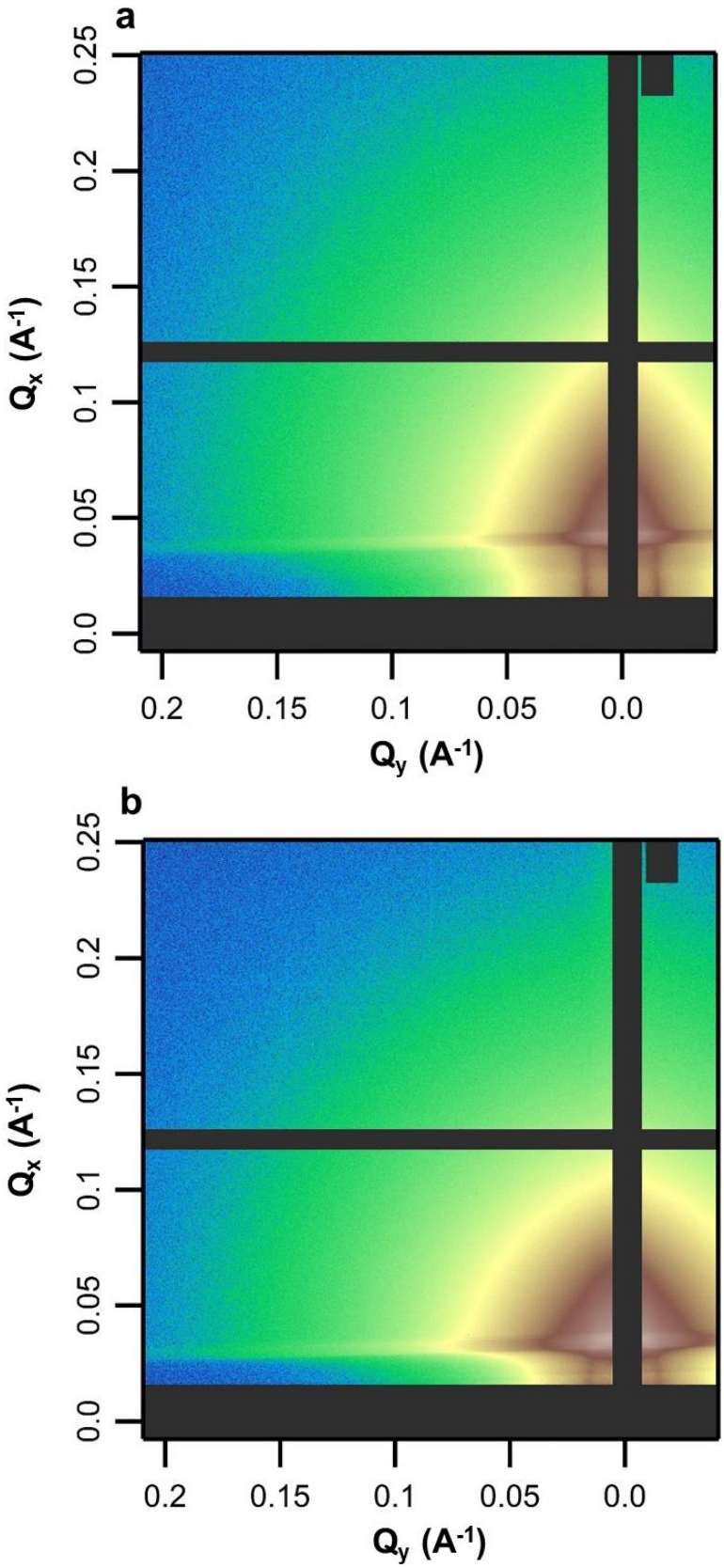

Figure S2: Grazing Incidence Small Angle X-Ray Scattering pattern for mesoporous (a) TiO_2 and (b) TiN.

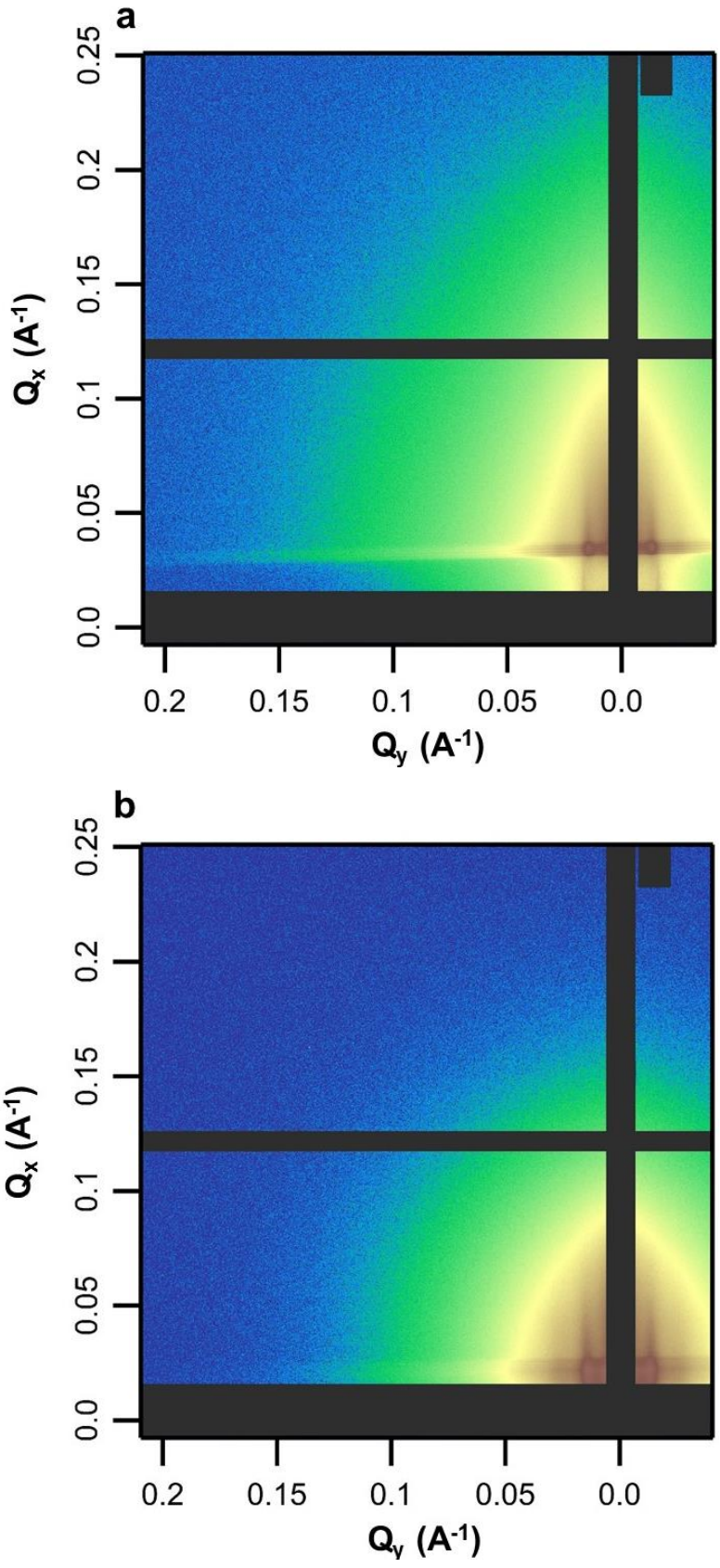

Figure S3: Grazing Incidence Small Angle X-Ray Scattering pattern for mesoporous (a) Nb_2O_5 and (b) NbN.

N_2-sorption Characterization

The total surface area of the oxide and nitride thin films was well below the detection limit for N_2-sorption, so monoliths with the same composition were used instead. Prior to analysis, the monoliths were crushed into a powder using a mortar and pestle. The surface area was determined using the Brunauer-Emmett-Teller (BET) method on a Micrometrics ASAP 2020 surface area and porosity analyzer at 77 K. Pore size distributions were also concurrently determined with the Barrett-Joyner-Halenda (BJH) method. All samples were degassed at 120 °C for six hours under vacuum prior to measurement.

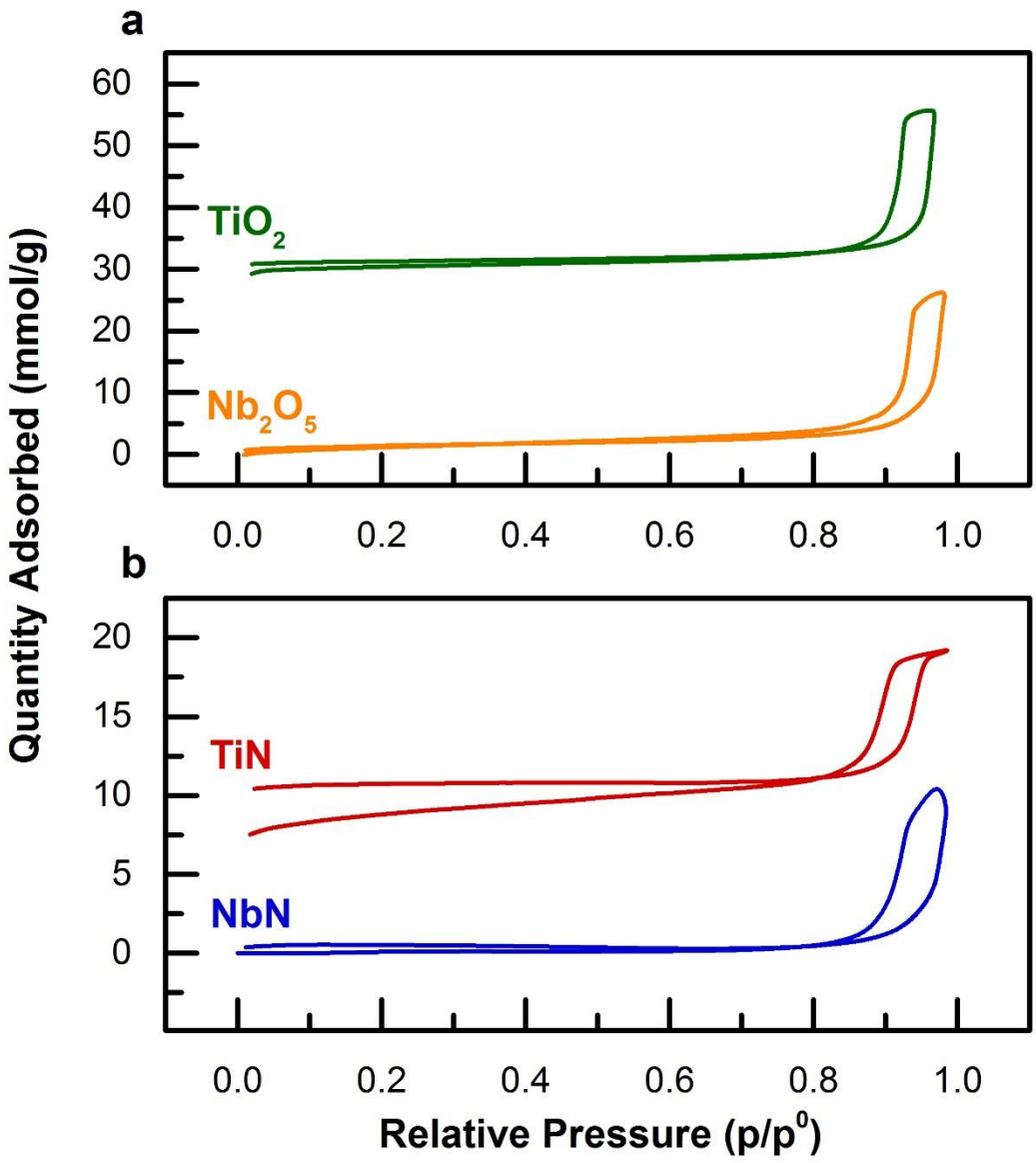

Figure S4: N_2-adsorption isotherms for mesoporous (a) oxides and (b) nitrides showing typical type IV curves with H_1-type hysteresis indicating that porosity is dominated by mesoporosity (2-50 nm pore size). For visual clarity, the TiO_2 curve has been offset by 30 mmol/g and the TiN curve has been offset by 10 mmol/g.

The monolith synthesis and processing steps were identical to the thin films except that the ISO terpolymer was dissolved in 6 mL THF and was cast in polytetrafluoroethylene (PTFE) dishes. Additionally, unlike the thin films, a dense capping layer is seen on the oxide/terpolymer hybrid monoliths. This layer was removed with CF_4 plasma using an Oxford Instruments PlasmaLab 80^+ with 300W RF power and a CF_4 flow rate of 30 sccm. Monoliths were treated for 40 minutes on each side to ensure complete capping layer removal.

Due to the slower drying kinetics, the oxide and nitride monoliths have additional long range order,[3,4] suggesting that the pore size and surface area results may not be identical to the thin films. However, the specific capacitance values for both the TiN and NbN thin films used the monolith surface area results and matched well with literature,[12,13] suggesting that any variations are small.

SEM Characterization

A TESCAN MIRA3 LM field-emission scanning electron microscope was used to analyze the morphology and pore structure of all nitride thin films. Films were adhered to stub mounts using carbon tape and coated with Au-Pd to increase the conductivity. The morphology was analyzed by observing the samples perpendicular to the plane of the film, while the film thickness was characterized using sample mounts with a 70° tilt.

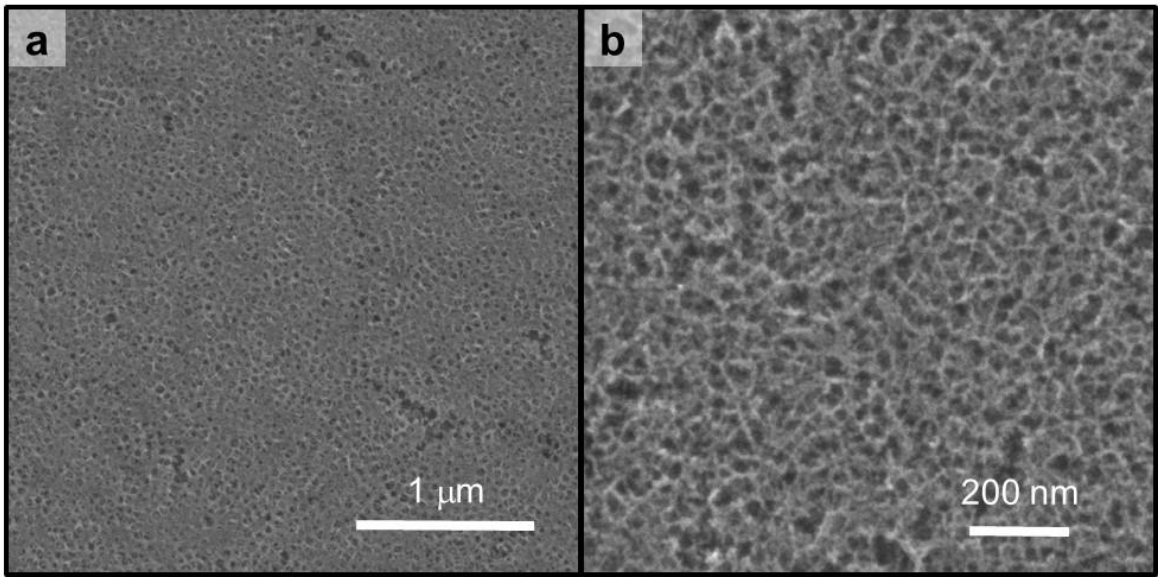

Figure S5: Top view SEM image of (a) amorphous Nb_2O_5 and (b) anatase TiO_2

Capacitance Results:

The capacitance of the porous TiN films is 25 F/g when scanned at 10 mV/s in 0.1 M $HClO_4$ electrolyte between 0.1 V and 1.4 V vs. RHE. Meanwhile, the NbN films have a capacitance of 15 F/g under the same conditions when scanned from -0.3 V to 0.85 V vs. RHE. We observe a slight scan rate dependence for both TiN and NbN, indicating that while the films are sufficiently conductive for use as catalyst supports, their conductivity is less than that of a pure metal.

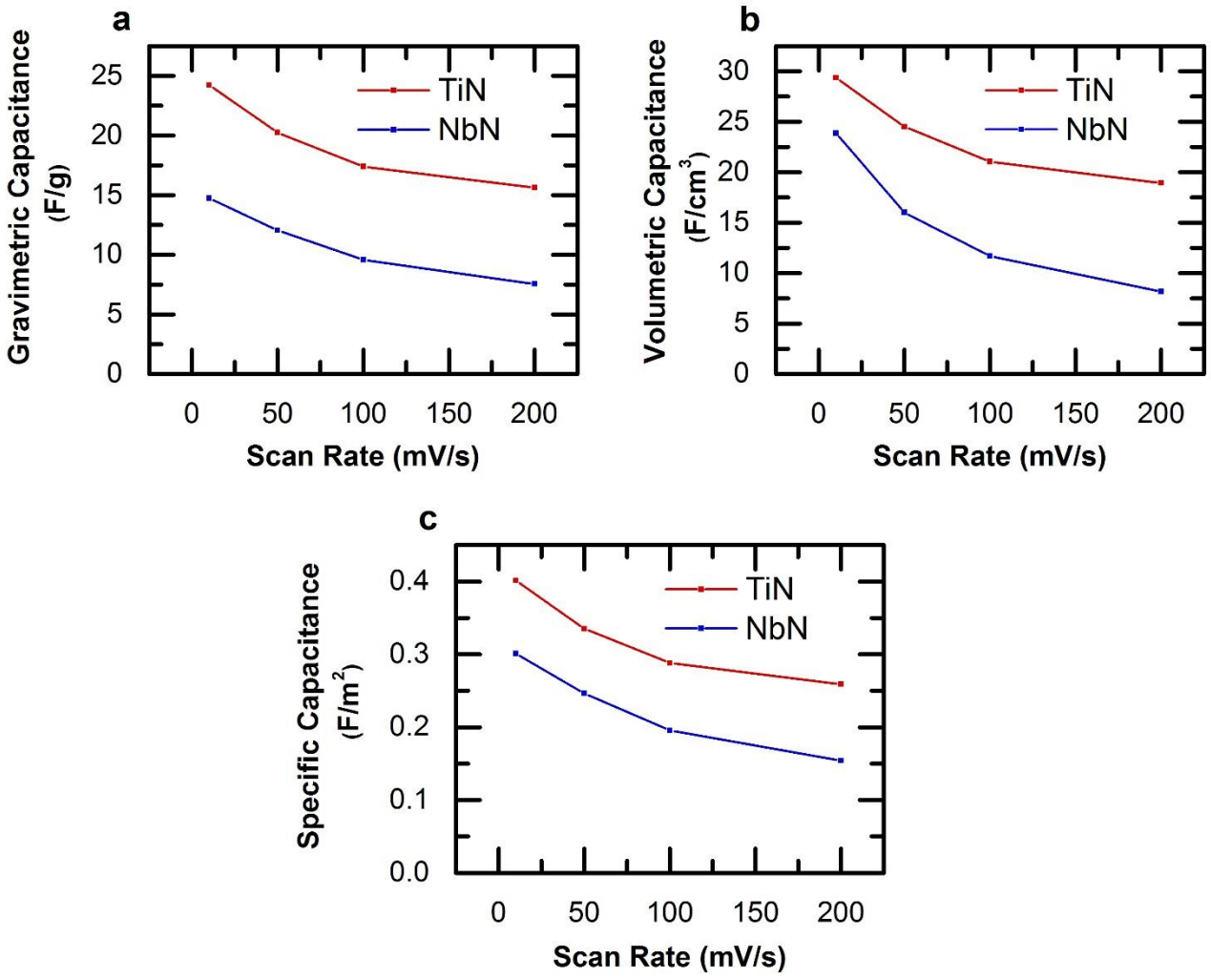

Figure S6: Scan rate dependence for TiN and NbN (a) gravimetric capacitance, (b) volumetric capacitance, and (c) specific capacitance.

Conductivity Results:

To confirm that charge transfer between the support and the electrolyte is not limited by the film conductivity, ferrocenemethanol was used as a redox probe. Since the iron(II)/iron(III) redox couple is kinetically facile, we assume that there is no kinetic overpotential associated with the redox transition. Therefore, the offset in the oxidation and reduction peaks can be attributed to overpotential associated with the electrical conductivity until the peak offset reaches the Nernstian limit of 59 mV. Note that the traditional ferri/ferrocyanide redox couple which is used to measure conductivity in alkaline conditions cannot be used in acidic electrolytes due to the formation of cyanide gas. Since there is no Fe^{3+} containing molecule in our system, no back redox couple is present, which necessitates that the electrolyte is kept free of disturbances to limit diffusion of the oxidized ferrocenemethanol molecules away from the electrode.

To confirm that ferrocenemethanol is a valid redox probe, a bare glassy carbon electrode was first tested in 0.1 M $HClO_4$ with 300 μM ferrocenemethanol. The resulting peak offset was consistent with the Nernstian limit, validating the use of ferrocenemethanol.

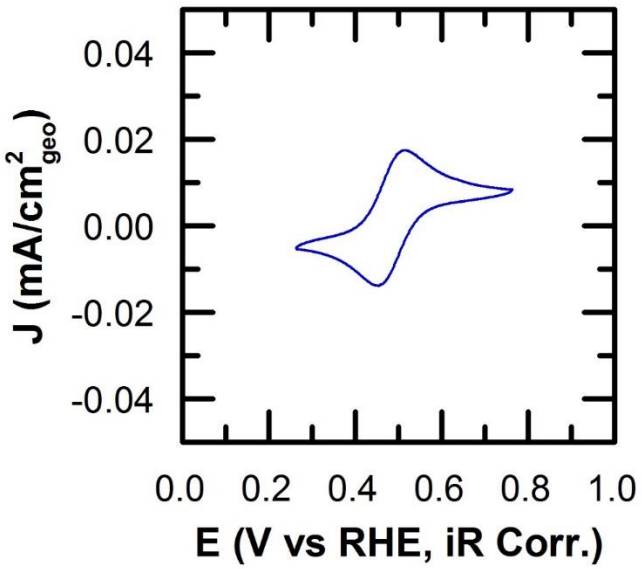

Figure S7: Iron(II)/Iron(III) redox couple on a glassy carbon electrode in 0.1 M $HClO_4$ electrolyte with 300 μM ferrocenemethanol scanned at 10 mV/s.

Subsequently, the mesoporous nitride films were analyzed using the same technique. In the case of TiN, the peak offset was consistent with the glassy carbon electrode both when cycled at low potential, as well as when cycled to 1.4 V, suggesting that TiN is stable to 1.4 V. Meanwhile, for NbN the initial peak offset was comparable to both the glassy carbon electrode as well as the TiN film. However, after cycling to high potential there were no redox peaks present for the NbN film, indicating that the surface of the film was electrochemically insulating.

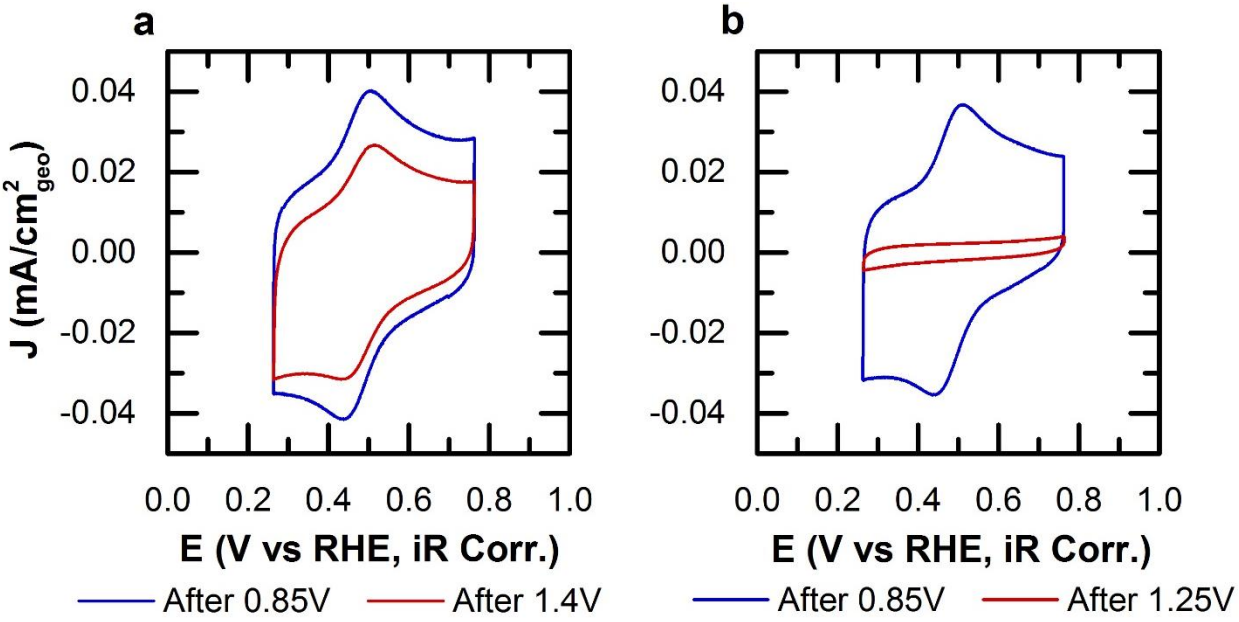

Figure S8: Iron(II)/Iron(III) redox couple on mesoporous (a) TiN and (b) NbN thin films in 0.1 M $HClO_4$ electrolyte with 300 μM ferrocenemethanol scanned at 10 mV/s

The NbN film showed a large oxidative current when cycled to high voltage, likely indicating the formation of a niobium oxide layer on the surface. This layer is likely the cause of the insulating nature of the NbN film after cycling to high potential.

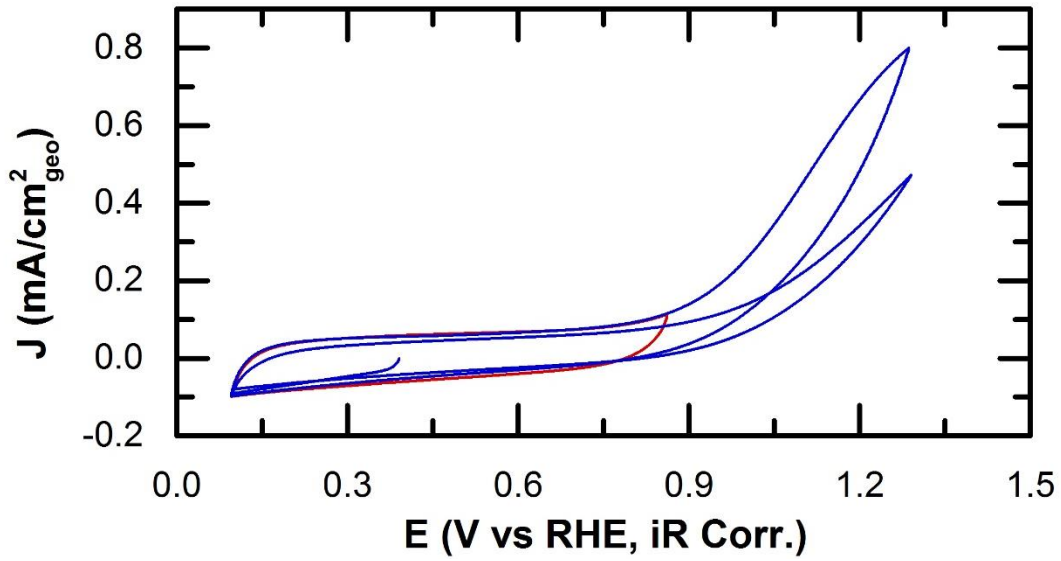

Figure S9: Mesoporous NbN thin film cyclic voltammogram in 0.1 M $HClO_4$ electrolyte scanned at 50 mV/s showing rapid oxidation when cycled to high voltage.

After 2,000 cycles to 1.4 V, the TiN film still showed a redox peak offset consistent with the initial value, indicating that the film conductivity was maintained under prolonged high potential exposure.

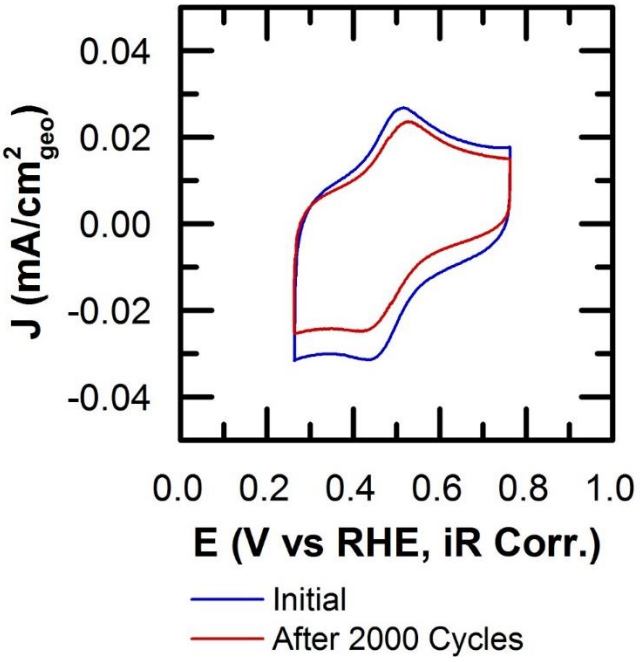

Figure S10: Iron(II)/Iron(III) redox couple on mesoporous TiN in 0.1 M $HClO_4$ electrolyte with 300 μM ferrocenemethanol scanned at 10 mV/s before and after durability test.

As additional confirmation of film conductivity, four-point probe conductivity measurements were taken using the van der Pauw method. First, Ti wires were polished to remove the surface oxide and were subsequently affixed to the corners of the films using conductive silver paint and allowed to cure for 2 h. After curing, an inert two-part epoxy was mixed and used to cover the silver paint, providing additional mechanical support. The inert epoxy was allowed to cure for 12 h.

The horizontal resistance was measured by taking the average along the two horizontal edges using both polarities of the current source and voltage meter. An analogous method was used to calculate the vertical resistance. The sheet resistance was calculated numerically from the horizontal and vertical resistance using the relation:

$$e^{-\pi R_{vertical}/R_{sheet}} + e^{-\pi R_{horizontal}/R_{sheet}} = 1 \quad (1)$$

Resistivity was determined by multiplying the sheet resistance by the thickness and the porosity fraction, while conductivity was calculated from the inverse of resistivity. The TiN films had a conductivity of 301.1 S/cm and the NbN films had a conductivity of 16.1 S/cm. These conductivity values are lower than bulk TiN and NbN likely due to residual oxygen resulting from the low ammonolysis temperature needed to maintain the porous structure but remain significantly higher than typical carbon supports.

References:

1 J. Allgaier, A. Poppe, L. Willner and D. Richter, *Macromolecules*, 1997, **30**, 1582–1586.

2 S. C. Warren, F. J. DiSalvo and U. Wiesner, *Nat. Mater.*, 2007, **6**, 156–161.

3 S. W. Robbins, P. A. Beaucage, H. Sai, K. W. Tan, J. G. Werner, J. P. Sethna, F. J. DiSalvo, S. M. Gruner, R. B. Van Dover and U. Wiesner, *Sci. Adv.*, 2016, **2**, 1–8.

4 S. W. Robbins, H. Sai, F. J. DiSalvo, S. M. Gruner and U. Wiesner, *ACS Nano*, 2014, **8**, 8217–23.

5 J.-G. Yu, H.-G. Yu, B. Cheng, X.-J. Zhao, J. C. Yu and W.-K. Ho, *J. Phys. Chem. B*, 2003, **107**, 13871–13879.

6 S. Venkataraj, R. Drese, C. Liesch, O. Kappertz, R. Jayavel and M. Wuttig, *J. Appl. Phys.*, 2002, **91**, 4863–4871.

7 Y. Shao-Horn, W. C. Sheng, S. Chen, P. J. Ferreira, E. F. Holby and D. Morgan, *Top. Catal.*, 2007, **46**, 285–305.

8 W. Sheng, S. Chen, E. Vescovo and Y. Shao-Horn, *J. Electrochem. Soc.*, 2012, **159**, B96–B103.

9 A. Taniguchi, T. Akita, K. Yasuda and Y. Miyazaki, *J. Power Sources*, 2004, **130**, 42–49.

10 B. Lim, M. Jiang, P. H. C. Camargo, E. C. Cho, J. Tao, X. Lu, Y. Zhu and Y. Xia, *Science (80-.).*, 2009, **324**, 1302–1305.

11 J. Ilavsky, *J. Appl. Cryst*, 2012, **45**, 324–328.

12 D. Choi and P. N. Kumta, *J. Am. Ceram. Soc.*, 2011, **94**, 2371–2378.

13 X. Tian, J. Luo, H. Nan, Z. Fu, J. Zeng and S. Liao, *J. Mater. Chem. A*, 2015, **3**, 16801–16809.